

STRUCTURAL AND ELECTRICAL PROPERTIES OF PEROVSKITES $\text{La}_{1-x}\text{Sr}_x\text{MnO}_3$ ($x=0,0.3$) SYNTHESIZED VIA SOL –GEL CITRATE METHOD

Archana B. Bodade¹, G.N. Chaudhari², Anjali B. Bodade³

Assistant Professor, Professor, Associate Professor

Department of Physics

Shri Shivaji Science College, Amravati (M.S), India.

Abstract: Nanocrystalline and nanocomposites of Sr doped $\text{La}_{1-x}\text{Sr}_x\text{MnO}_3$ ($x=0,0.3$) were synthesised by the sol –gel citrate method. Structural and dielectric analysis were performed for synthesized nanocomposites $\text{La}_{1-x}\text{Sr}_x\text{MnO}_3$. The XRD of $\text{La}_{1-x}\text{Sr}_x\text{MnO}_3$ ($x=0,0.3$) shows orthorhombic structure. Dielectric constant (ϵ' and ϵ'') of $\text{La}_{1-x}\text{Sr}_x\text{MnO}_3$ ($x=0,0.3$) were measured as a function of frequency in the range 42 Hz to 500 MHz and the temperature range 30 to 700°C. A ferroelectric like dielectric constant ranging from 10^4 to 10^6 was obtained for both. AC conductivity has been studied as a function of frequency and temperature to understand the conduction mechanism.

Key words: Nanocomposites of $\text{La}_{1-x}\text{Sr}_x\text{MnO}_3$, sol–gel, Electrical Conductivity, Dielectric Properties.

Introduction:

Nanotechnology is the engineering of systems and materials at the molecular scale. As far as nanomaterials are concerned, LaMnO_3 is one of the candidates which has been attracting actual interest of LaMnO_3 nanomaterial in chemistry and solid state physics is due to its excellence in electrical and optical properties [1]. LaMnO_3 (LMO) is an inorganic compound with perovskite structure. It is an A-type antiferromagnetic insulator with a low Neel temperature [2–5]. Depending on the synthesis process, LMO samples can be obtained as thin films [6], monocrystals [4,7] and polycrystalline powders [8].

When lanthanum ions (La^{3+}) in lanthanum manganese oxide (LaMnO_3) are partially substituted with divalent ions like Sr^{2+} , a mixed valence state of $\text{Mn}^{3+}/\text{Mn}^{4+}$ is generated, leading to a number of spectacular physical properties, such as insulating to metal transition, colossal magneto resistance, and paramagnetic to ferromagnetic transition [9]. The electrical magnetic characteristics of (La, Sr) MnO_3 (LSMO) can be tuned per device requirements by changing Sr dopant concentration in LSMO. As a result, LSMO has potential applications in various magnetic devices including magnetic field sensors and recording devices [10].

The present work is an attempt to study the electrical properties (dielectric and ac conductivity) of $\text{La}_{1-x}\text{Sr}_x\text{MnO}_3$ ($x=0, 0.3$) ceramic prepared by sol-gel method.

2. Experimental

Polycrystalline $\text{La}_{1-x}\text{Sr}_x\text{MnO}_3$ ($x=0,0.3$) were prepared using sol–gel method. High purity nitrates were used for the preparation. A stoichiometric mixture lanthanum nitrate and manganese nitrate and strontium were used as raw materials. A stoichiometric mixture of nitrates was mixed with citric acid and ethylene glycol and stirred magnetically at 80°C for 3h to obtain a homogenous mixture; the solution was further heated in a pressure vessel at about 130°C for 12 hrs and subsequently kept at 350°C for 3 hrs a muffle furnace and then milled to a fine powder. The dried powder was then calcined in the range of 350°C to 750°C for 6 hrs in order to improve the crystallinity of the powder. The dielectric measurement were done on the pellets (the pellets of 13.2 mm diameter and 15.45 mm thickness were made by

applying a pressure of 8 tons on the powered sample) by using an LCR meter. Dielectric measurement were carried out in the frequency range 42 Hz-500 MHz and at temperature range 35 to 700°C

3 .Result and Discussion:

3.1 Structural Analysis

The XRD patterns of the precursor powders LaMnO_3 and dopped $\text{La}_{0.7}\text{Sr}_{0.3}\text{MnO}_3$ calcined at 550°C for 6 h are shown in Figure 1.

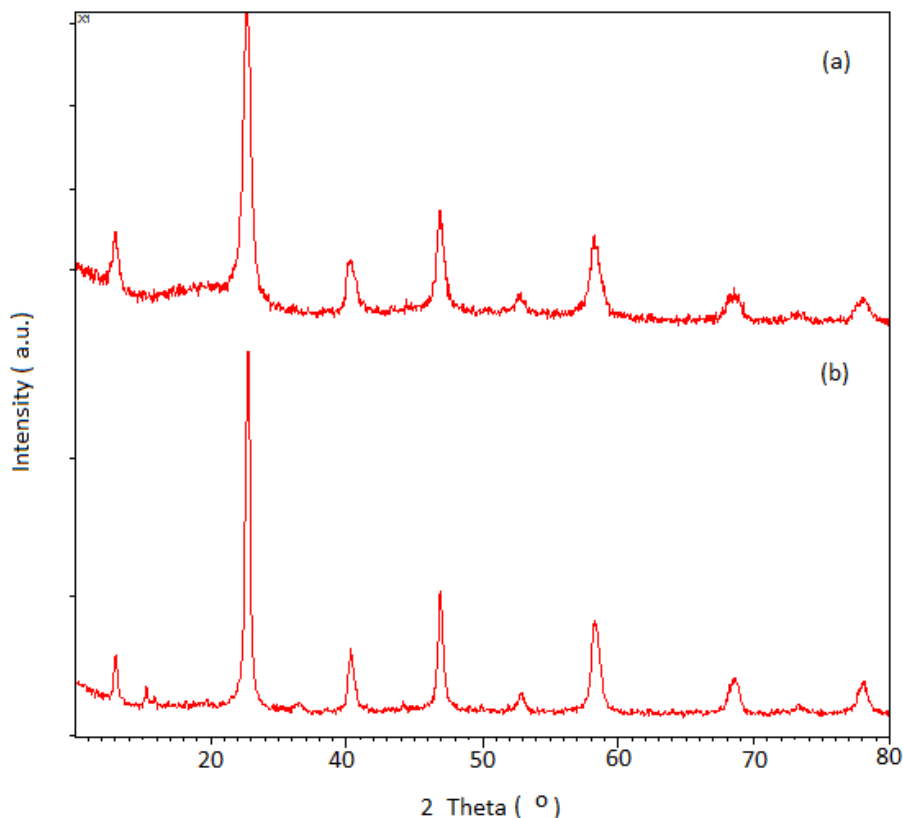


figure1:XRD patterns of the (a) LaMnO_3 , (b) $\text{La}_{0.7}\text{Sr}_{0.3}\text{MnO}_3$ synthesis by sol-gel citrate method at 550°C

Figure 1(a), shows the XRD pattern of LaMnO_3 . All the diffraction peaks of the phases are indexed as perovskite-type with orthorhombic structure. The diffraction data are in good agreement with JCPDS card of LaMnO_3 (JCPDS No .50-029). Figure 1(b), shows the XRD pattern of nanomaterial, which indicates that ions Sr^{2+} partially substitute for La^{3+} ions in the LaMnO_3 crystal lattice. The ionic radii of Sr^{2+} (1.21 Å) are very close to that of La^{3+} and Sr is incorporated into the LaMnO_3 lattice at the La site. The mean crystallite sizes (D) of $\text{La}_{0.7}\text{Sr}_{0.3}\text{MnO}_3$ powder was deduced from half height width of XRD peaks based on the Scherrer's equation, $t = 0.9\lambda/\beta\cos\theta$, where t is the average size of the particles, λ is wavelength of X-ray radiation, β the full width at half maximum of the diffracted peak and θ is the angle of diffraction [11]. Extremely broad reflections are observed indicating nano- sized particle nature of the material obtained. The average particle size of the nanocrystalline $\text{La}_{0.7}\text{Sr}_{0.3}\text{CrO}_3$ according to the Scherrer formula was in the range of 30 - 35 nm.

3.2. Surface Morphology

The TEM micrographs, Fig. 2 (a-b) shows particle size and shape morphology of LaMnO_3 and $\text{La}_{0.7}\text{Sr}_{0.3}\text{MnO}_3$ nanoparticles calcined at 550°C . The image reveals that the sample consist of spherical particles with the average size of 60 nm and 45 nm which is in close agreement with that estimated by Scherer formula based on the XRD pattern

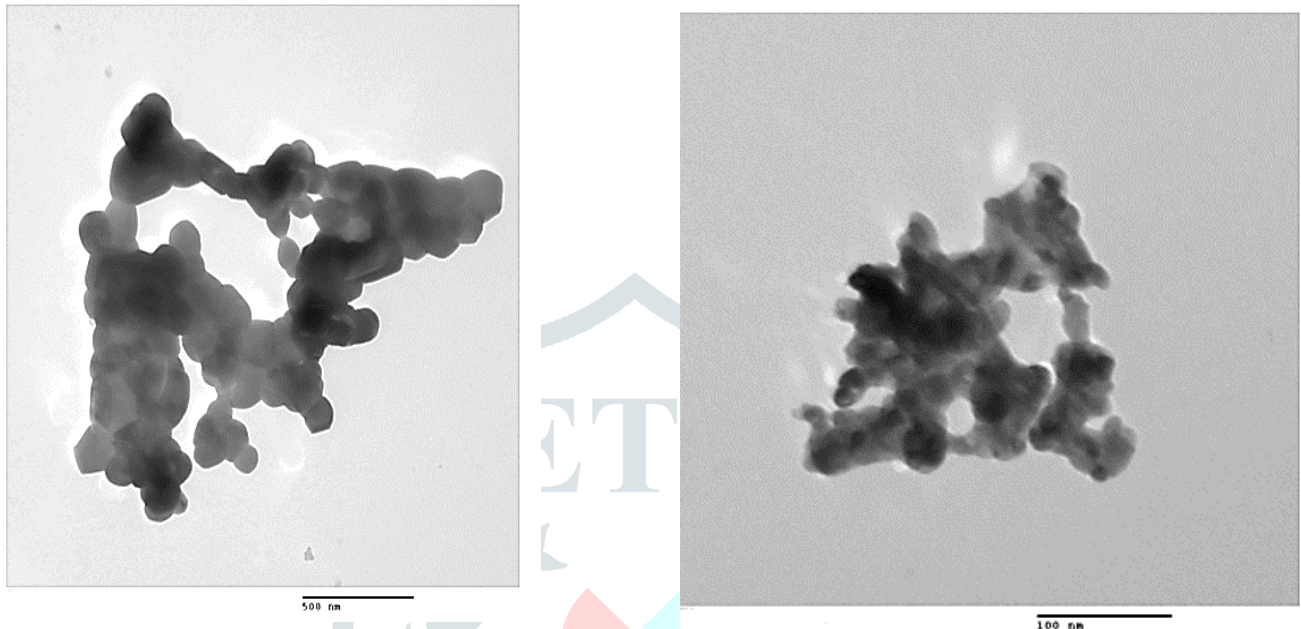


figure 2 (a): TEM image of LaMnO_3 calcined at 550°C figure2 (b) TEM micrograph of $\text{La}_{0.7}\text{Sr}_{0.3}\text{MnO}_3$ calcined at 550°C

3.3 Dielectric analysis

Figure 3(a-b) shows value of dielectric constant decreasing with increase in frequency for pure and substituted samples at higher temperatures. This happens due to the presence of all types of polarizations (i.e. interfacial, ionic, dipolar, electronic and space charge) [12 -14]. At higher frequencies, the main contribution to dielectric constant comes from electronic polarization, as some of the polarizations become ineffective and thus, the value of dielectric constant decreases. A plot of ϵ'' vs. frequency indicates a strong frequency and temperature dependence with power law behaviour is shown in Fig. 4(a-b). The exponential behaviour of ϵ'' vs. frequency shows an insulator (or semiconductor-) characteristic, which suggests that the low frequency enhancement of ϵ'' is related to loosely bound charges. These results are similar to the dielectric response of LaSrFeO_3 [15]

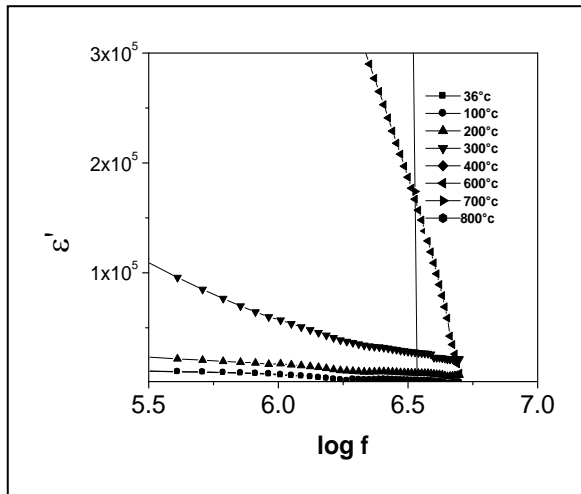


fig.3 (a) LaMnO₃

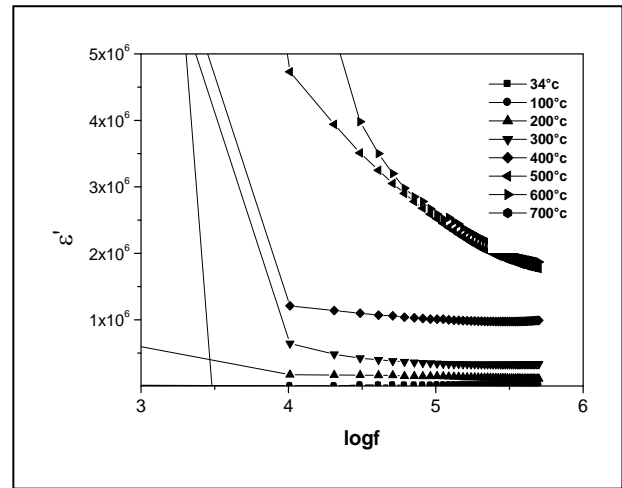


fig.3 (b) La_{0.7}Sr_{0.3}MnO₃

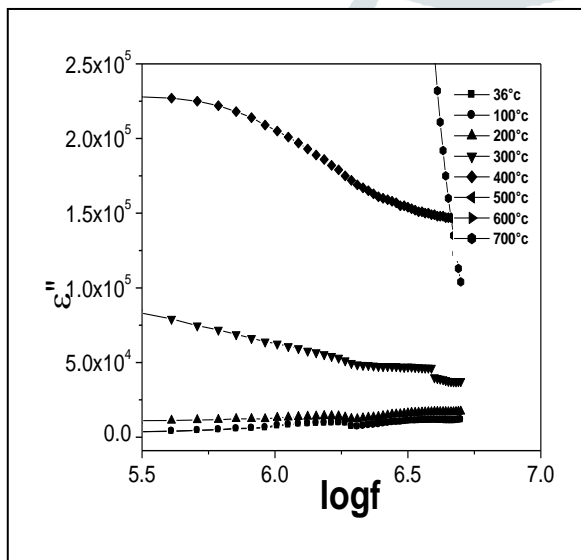


fig.4(a) LaMnO₃

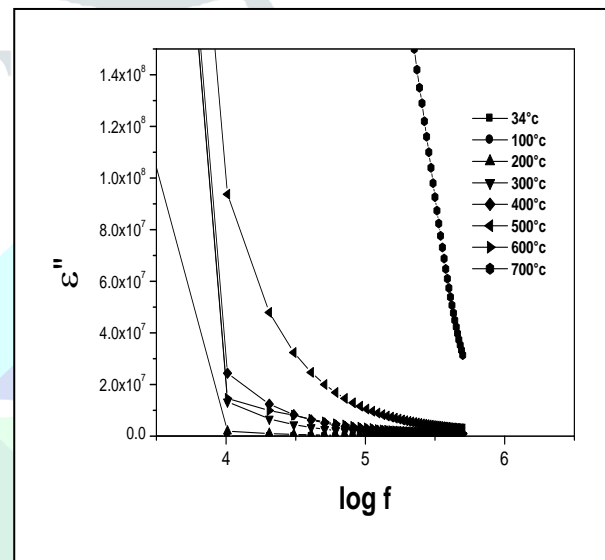


fig.4 (b) La_{0.7}Sr_{0.3}MnO₃

fig[3(a-b)]Real part of the dielectric constant as a function of frequency for LaMnO₃and La_{0.7}Sr_{0.3}MnO₃ and fig[4(a-b)] imaginary part of the dielectric constant as a function of frequency for LaMnO₃ and La_{0.7}Sr_{0.3} MnO₃

3.4 AC CONDUCTIVITY

The ac electrical conductivity was obtained using the relation:

$$\sigma_{ac} = l/SZ' \text{ ----- (1)}$$

where l is the thickness and S is the surface area of the specimen. The variation of σ_{ac} of for LaMnO₃ and La_{0.7}Sr_{0.3} MnO₃ as a function of frequency at different temperature is shown in [fig5 (a-b)]. At low temperature σ_{ac} varies linearly with frequency .The frequency variation of σ_{ac} involves a power exponent ($\sigma_{ac} \propto \omega^n$, n is

the exponent and can assume the value <1 and ω is angular frequency of a.c. field). This indicates that conduction process is thermally activated process. At high temperature, frequency independent a.c. conductivity is observed in low frequency region. This frequency independent region increases with increase in temperature and obeys the following phenomenological law [16]

$$\sigma_{ac} = \sigma_{dc} + A \cdot \omega^n \quad (2)$$

with $0 \leq n \leq 1$ and A is thermally activated quantity and σ_{dc} the frequency independent (dc) part of conductivity. Also it is observed that the electrical conductivity increases with increase in temperature. A similar behaviour was observed in $(\text{Na}_{0.5}\text{Bi}_{0.5})\text{ZrO}_3$ ceramic [17,18].

Figure 5(c-d) shows variation of a.c. conductivity vs inverse temperature of LaMnO_3 and $\text{La}_{0.7}\text{Sr}_{0.3}\text{MnO}_3$ ceramic at various frequency. The a.c. conductivity ($\sigma_{a.c.}$) of the above ceramic materials can be calculated by using the relation

$$\sigma_{a.c.} = \omega \varepsilon_0 \varepsilon_r \tan \delta \quad (3)$$

where $2\pi f = \omega$, ε_0 is the permittivity of free space, ε_r the relative dielectric constant, $\tan \delta$ the dissipation factor [19, 20, 21]. The a.c. conductivity pattern indicates a progressive rise in conductivity with rise in temperature at a various frequency. A frequency independent relation between a.c. conductivity and temperature is studied as

$$\sigma = \sigma_0 \exp(-E_a/k_B T) \quad (4)$$

where σ_0 is a constant, k_B the Boltzmann constant and E_a the activation energy for conduction [22-23]. The value of activation energy decreases with increase in temperature and also activation energy decreases with increase in temperature for Sr substitutions. All the activation energies at various frequency for LaMnO_3 and $\text{La}_{0.7}\text{Sr}_{0.3}\text{MnO}_3$ are recapitulated in table 1. This type of temperature dependent in a.c. conductivity indicates that the electrical conduction in the materials a thermally-activated process.

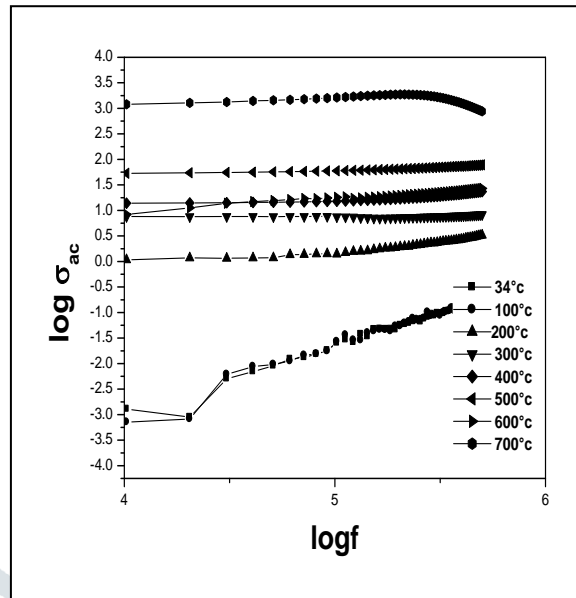
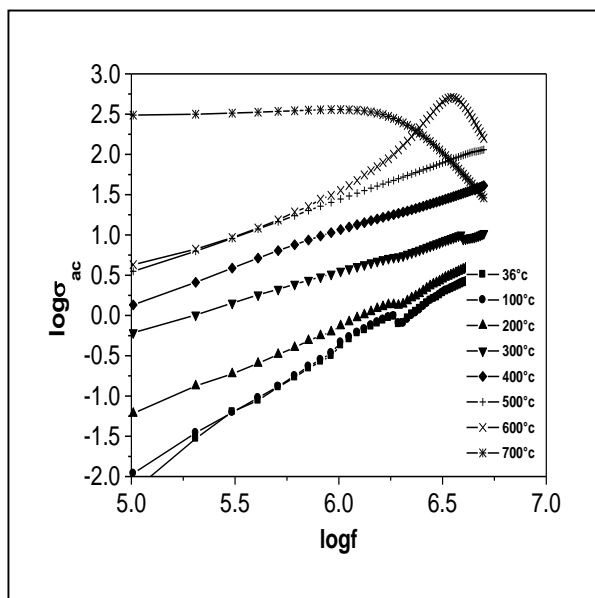


Fig5(a)

Fig5(b)

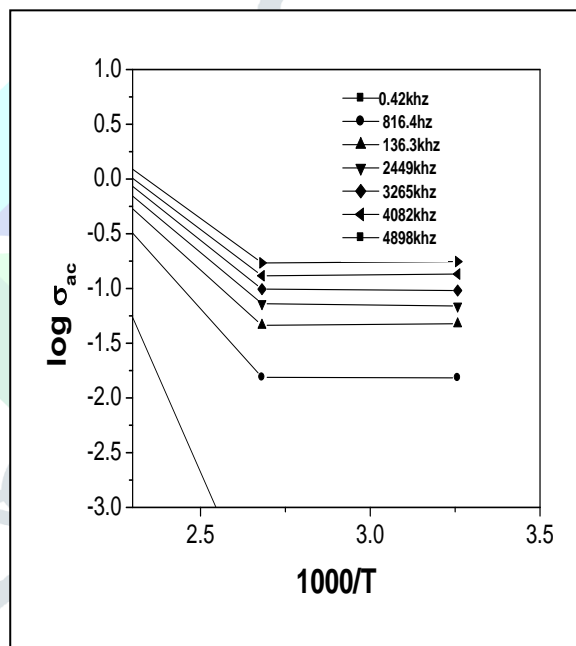
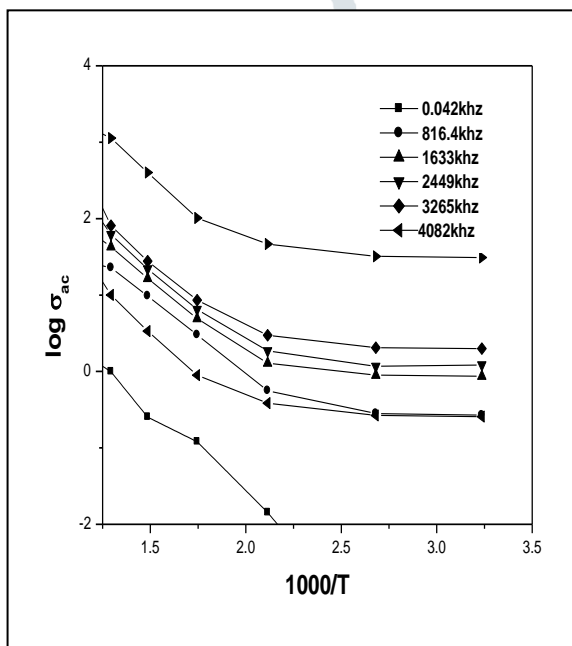


Fig5 (c)

Fig5(d)

Fig.5(a,b) Frequency-dependent ac conductivity(σ_{ac}) of LaMnO_3 and $\text{La}_{0.7}\text{Sr}_{0.3}\text{MnO}_3$ at various temperatures and Fig.5(c,d) Arrhenius plot of LaMnO_3 and $\text{La}_{0.7}\text{Sr}_{0.3}\text{MnO}_3$ at various frequencies

Table 1 :Activation energies of LaMnO_3 and $\text{La}_{0.7}\text{Sr}_{0.3}\text{MnO}_3$ at various frequency range

Frequency Range	Activation Energy	
	LaMnO_3	$\text{La}_{0.3}\text{Sr}_{0.7}\text{MnO}_3$
42 Hz	2.9×10^{-3}	7.7×10^{-4}
81.6 Hz	1.1×10^{-4}	1.7×10^{-4}
163.3 Hz	9.6×10^{-5}	1.57×10^{-5}
244.9 Hz	8.7×10^{-5}	1.50×10^{-5}
326.5 Hz	8.6×10^{-5}	1.43×10^{-5}
408.2 Hz	7.67×10^{-5}	1.36×10^{-5}
489.8 Hz	6.53×10^{-5}	1.30×10^{-5}

Conclusion : Polycrystalline sample of $\text{La}_{1-x}\text{Sr}_x\text{MnO}_3$ ($x=0, 0.3$) perovskite ceramics have been prepared by using sol-gel technique. The XRD pattern of $\text{La}_{0.7}\text{Sr}_{0.3}\text{MnO}_3$ shows perovskite-type with orthorhombic structure. The results revealed that the particle size is in the range of 30 - 35 nm for $\text{La}_{0.7}\text{Sr}_{0.3}\text{MnO}_3$ with good crystallinity. From the result obtained a small amount of ($x = 0.3$) Sr doping in $\text{La}_{1-x}\text{Sr}_x\text{MnO}_3$ changes the complex dielectric constant substantially as shown in [Fig. 1(a-b)] and [Fig(2c-d)]. Although the strong frequency and temperature dependence is qualitatively similar to that of LaMnO_3 , the absolute values increase by a factor of 1000 in both ϵ' and ϵ'' , from 10^5 to 10^6 and 10^5 to 10^8 , respectively. From conductivity analysis, we observed that the value of activation energy decreases with increase in frequency for Sr substitutions. The ac conductivity was found to obey the universal power law. The pair approximation type correlated barrier hopping (CBH) model successfully explained the universal behaviour of exponent n . Also, the frequency dependent ac conductivity at different temperatures indicated that the conduction process is thermally activated process.

Acknowledgement

Authors are very much thankful to Dr.V.G.Thakare, Principal, Shri Shivaji Science College, Amravati for providing the necessary laboratory facilities.

References :

- [1] <http://www.Nano Technology and Non woven .com>
- [2] Wenwei W, Jinchao C, Xuehang W, Sen L, Kaituo W, Lin T. Nanocrystalline LaMnO_3 preparation and kinetics of crystallization process. Adv Powder Technol 2013;24:154–9.

- [3] Zhao J, Song T, Kunkel H, Zhou X, Roshko R, Williams G. *La_{0.95}Mg_{0.05}MnO₃: an ideal ferromagnetic system?* J Phys:Condens Matter 2000;12:6903.
- [4] Rodríguez-Carvajal J, Hennion M, Moussa F, Moudden AH, Pinsard L, Revcolevschi A. Neutron-diffraction study of the Jahn-Teller transition in stoichiometric LaMnO_3 . *Phys Rev B* 1998;57(6):3189.
- [5] Zhong-Qin Y, Qiang S, Ling Y, Xi-De X. A discrete variational method study on the electronic structures of CaMnO_3 and LaMnO_3 . *Acta Phys Sin-Ov Ed* 1998;7(11):851.
- [6] Khanduri H, Chandra Dimri M, Vasala S, Leinberg S, Lohmus R, Ashworth TV, et al. Magnetic and structural studies of LaMnO_3 thin films prepared by atomic layer deposition. *J Phys D: Appl Phys* 2013;46:175003.
- [7] Zhou J-S, Goodenough JB. Paramagnetic phase in single-crystal LaMnO_3 . *Phys Rev B* 1500;60(22):2.
- [8] Kitayama K. Phase equilibrium in the system Ln–Mn–O: I. Ln = La at 1100°C. *J Solid State Chem* 2000;153:336–41.
- [9] C. Martínez-Boubeta, Z. Konstantinovic, L. Balcells, S. Estrade, J. Arbiol, A. Cebollada, and B. Martinez, *Cryst. Growth Des.* **10**, 1017 (2010).
- [10] R. Desfeux, S. Bailleul, A. Da Costa, W. Prellier, and A. M. Haghiri-Gosnet, *Appl. Phys. Lett.* **78**, 3681 (2001).
- [11] B. D. Cullity, “Elements of X-Ray Diffraction,” 2nd Edition, Addison Wesley, New York, 1978, pp. 155-165.
- [12] Chua B W, Lu L, Lai M O and Wong G H L 2005 *J. Alloys Compd.* **386** 303
- [13] Ranjan R, Kumar Kalyani A, Garg R and Krishna P S R 2009 *Solid State Commun.* **149** 2008
- [14] Vijendra Chaudhari A and Bichile G K 2010 *Physica B* **405** 534
- [15] G. Chern, W. K. Hsieh, M. F. Tai, and K. S. Hsung, *Phys. Rev. B* 58, 1252 (1998).
- [16] Jonscher K, *Nature*, 267 (1977) 673
- [17] Lily, Kumari K, Prasad K and Yadav K, *J Mater Sci*, 42 (2007) 6252
- [18] Elliott S R, *Philos Mag B*, 37 (1978) 553
- [19] Pradhan D K, Choudhary R N P, Rinaldi C and Katiyar R S 2009 *J. Appl. Phys.* 106 024102
- [20] Tiwari B and Choudhary R N P 2009a *Solid State Sci.* **11** 219
- [21] Tiwari B and Choudhary R N P 2009b *Physica B* 404 4111
- [22] Kumar M and Yadav K L 2007 *J. Phys. Condens. Matter* **19** 242
- [23] Shukla A and Choudhary R N P 2010 *Physica B* **405** 2508